PID+ BACKSTEPPING CONTROL OF RELATIVE SPACECRAFT ATTITUDE

Thomas R. Krogstad [*] **Raymond Kristiansen** [**]
Jan Tommy Gravdahl [*]

[*] *Dept. of Engineering Cybernetics, Norwegian University of Science and Technology, NO-7491 Trondheim, Norway*
[**] *Dept. of Computer Science, Electrical Engineering and Space Technology, Narvik University College, NO-8505 Narvik, Norway*

Abstract: In this paper we present a PID+ backstepping controller, as a solution to the problem of coordinated attitude control in spacecraft formations. The control scheme is based on quaternions and modified Rodriguez parameters as attitude representation of the relative attitude error. Utilizing the invertibility of the modified Rodriguez parameter kinematic differential equation, a globally exponentially stable control law for the relative attitude error dynamics is obtained through the use of integrator augmentation and backstepping. Finally, simulation results are presented to show controller performance.

Keywords: Attitude control, formation control, modified Rodriguez parameters

1. INTRODUCTION

Formation flying missions and missions involving coordinated control of several autonomous vehicles have been areas of increased interest in later years. This is due to the many inherent advantages the distributed design adds to the mission. By distributing payload on several spacecraft, redundancy is added to the system, minimizing the risk of total mission failure, several cooperating spacecraft can solve assignments which are more difficult and expensive, or even impossible with a single spacecraft, and the launch costs may be reduced since the spacecraft can be distributed on more inexpensive launch vehicles. A condition for formation flight is however a fully autonomous vehicle, as controlling spacecraft in close formation is only possible using automatic control. This results in stringent requirements on control algorithms and measurement systems.

Several control objectives can be defined depending on the specific mission of the formation. Missions may be divided into Earth observation and Space observation. Earth observation missions include missions such as Synthetic Aperture Radar (SAR) missions, where the use of a formation increases the achievable resolution of the data. In SAR missions the control objective is usually to point the payload at the same location on Earth, involving keeping the relative attitude either constant or tracking a time-varying signal depending on formation configuration and satellite orbit. Examples of planned missions are TanDEM-X and SAR-LupeSpace observation missions focus on astronomical and astrophysical. The control objective usually involves keeping a constant absolute attitude in an inertial stellar system and to keep relative attitudes fixed. Examples of planned missions are XEUS and DARWIN.

Noticeable contributions on formation control may be divided in to three separate approaches: leader-follower, behavioral and virtual structure.

In the leader-follower strategy, one spacecraft is defined as leader of the formation while the rest are defined as followers. The control objective is to enable the followers to keep a fixed relative attitude with respect to the leader (Pan and Kapila, 2001; Kang and Yeh, 2002; Nijmeijer and Rodriguez-Angeles, 2003).

The behavioral strategy views each vehicle of the formation as an agent and the control action for each agent is defined by a weighted average of the controls corresponding to the desired behaviors for the agent. This approach eases the implementation of conflicting or competing control objectives, such as tracking versus avoidance. It is however difficult to enforce group behavior, and to mathematically guarantee stability and formation convergence. In addition, unforseen behavior may occur when goals are conflicting. This strategy is widely reported for use on mobile robots (Balch and Arkin, 1998) and (Mali, 2002), and was also applied to spacecraft formations in Lawton (2000).

In the virtual structure approach, the formation is defined as a virtual rigid body. In this approach the problem is how to define the desired attitude and position for each member of the formation such that the formation as a whole moves as a rigid body. In this scheme it is easy to prescribe a coordinated group behavior and to maintain the formation during maneuvers. But the actual performance is however dependent on the individual member's control system's ability to track the desired trajectories. Virtual structures were applied to mobile robots in (Lewis and Tan, 1997) and more recently to spacecraft formations in Beard *et al.* (2001) and Ren and Beard (2004).

In this paper, we present a PID+ tracking controller for relative attitude in a spacecraft formation. In the design, we utilize the advantages of the modified Rodriguez parameter kinematic to obtain a globally exponentially stable relative attitude error dynamics. The use of the MRP for control of attitude has previously been reported in Tsiotras (1996), and this work extends this approach to case of spacecraft formation coordination and by including integral action to counter constant perturbations, along the lines of what was reported in Fossen (2002).

The paper is organized as follows: Section 2 gives a general introduction to modeling and equations of motion, in Section 3 we propose and prove our main idea, then we include a simulation of a 2 satellite formation in Section 4 and conclusions are made in 5.

2. MODELING

In this section we give the equations of motion for a spacecraft actuated by means of thrusters, using the notation of Egeland and Gravdahl (2002) and Hughes (1986).

2.1 *Cartesian Coordinate Frames*

The coordinate reference frames used throughout the paper are shown in Fig. 1 and defined as follows:

2.1.1. *Earth Centered Inertial (ECI) Frame*

This frame is denoted $\mathcal{F}_i$, and has its origin located in the center of the Earth. Its z axis is directed along the rotation axis of the Earth towards the celestial north pole, the x axis is directed towards the vernal equinox, and finally the direction of the y axis completes a right handed orthogonal frame.

2.1.2. *Leader Orbit Reference Frame*

The leader orbit frame, denoted $\mathcal{F}_l$, has its origin located in the center of mass of the leader spacecraft. The $\mathbf{e}_r$ axis in the frame is parallel to the vector $\mathbf{r}_l$ pointing from the center of the Earth to the spacecraft, and the $\mathbf{e}_h$ axis is parallel to the orbit momentum vector, which points in the orbit normal direction. The $\mathbf{e}_\theta$ axis completes the right-handed orthogonal frame. The basis vectors of the

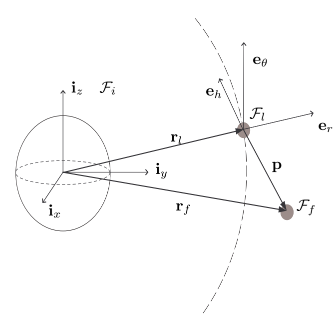

Fig. 1. Reference coordinate frames (Schaub and Junkins, 2003).

frame can be defined as

$$\mathbf{e}_r = \frac{\mathbf{r}_l}{r_l}, \qquad \mathbf{e}_\theta = \mathbf{e}_h \times \mathbf{e}_r \qquad \text{and} \qquad \mathbf{e}_h = \frac{\mathbf{h}}{h}, \tag{1}$$

where $\mathbf{h} = \mathbf{r}_l \times \dot{\mathbf{r}}_l$ is the angular momentum vector of the orbit, and $h = |\mathbf{h}|$.

2.1.3. *Follower Orbit Reference Frame*

This frame has its origin in the center of mass of the follower spacecraft, and is denoted $\mathcal{F}_f$. The vector pointing from the center of the Earth to the center of the follower orbit frame is denoted $\mathbf{r}_f$. Its origin is specified by a relative orbit position vector $\mathbf{p} = [x\ y\ z]^\top$ expressed in $\mathcal{F}_l$ frame components, as shown in Fig. 1, and the frame unit vectors align with the basis vectors of $\mathcal{F}_l$. Accordingly,

$$\mathbf{p} = \mathbf{r}_f - \mathbf{r}_l = x\mathbf{e}_r + y\mathbf{e}_\theta + z\mathbf{e}_h\,. \tag{2}$$

2.1.4. *Body Reference Frames* For both the leader and the follower spacecraft, body reference frames are defined and denoted $\mathcal{F}_{lb}$ and $\mathcal{F}_{fb}$, respectively. These frames have, similar to the orbit frame, the origin located in the center of mass of the respective spacecraft, but the basis vectors are fixed in the spacecraft body and coincide with its principal axis of inertia.

2.2 *Coordinate Frame Transformations*

2.2.1. *Rotation from ECI to Leader Orbit Frame* The rotation from the ECI frame to the leader orbit frame is dependent on the parameters of the leader spacecraft orbit, and can be expressed by three consecutive rotations. The total rotation matrix can be written ((Sidi, 1997))

$$\mathbf{R}_i^l = \mathbf{R}_{z,\omega+\nu}\mathbf{R}_{x,i}\mathbf{R}_{z,\Omega}, \tag{3}$$

where Ω is the right ascension of the ascending node of the orbit, i is the inclination of the orbit, ν is the true anomaly of the leader orbit, and ω is the argument of perigee of the same. The sum of ν and ω represents the location of the spacecraft relative to the ascending node. For the definitions of orbital parameters, consult testbooks on astrodynamics, such as Schaub and Junkins (2003).

2.2.2. *Body Frame Rotation* The rotation matrix describing rotations from an orbit frame to a body frame can be described by

$$\mathbf{R}_s^{sb} = [\mathbf{c}_1\ \mathbf{c}_2\ \mathbf{c}_3] = \mathbf{I}{+}2\eta_s\mathbf{S}\left(\boldsymbol{\epsilon}_s\right) + 2\mathbf{S}^2\left(\boldsymbol{\epsilon}_s\right) \tag{4}$$

where the elements $\mathbf{c}_i$ are directional cosines, and

$$\mathbf{q}_s = \left[\,\eta_s\ \ \boldsymbol{\epsilon}_s^\top\,\right]^\top \tag{5}$$

are the Euler parameters, which satisfy the constraint

$$\eta_s^2 + \boldsymbol{\epsilon}_s^\top\boldsymbol{\epsilon}_s = 1\,. \tag{6}$$

The superscript/subscript $s \in \{l, f\}$ will be used in general to denot the spacecraft in question. The matrix $\mathbf{S}\left(\cdot\right)$ is the cross product operator given by

$$\mathbf{S}\left(\boldsymbol{\epsilon}\right) = \begin{bmatrix} 0 & -\epsilon_z & \epsilon_y \\ \epsilon_z & 0 & -\epsilon_x \\ -\epsilon_y & \epsilon_x & 0 \end{bmatrix} \tag{7}$$

when $\boldsymbol{\epsilon} = [\epsilon_x\ \epsilon_y\ \epsilon_z]^\top$. The inverse rotation is given by the complex conjugate of $\mathbf{q}$ as

$$\bar{\mathbf{q}} = \left[\,\eta\ \ -\boldsymbol{\epsilon}^\top\,\right]^\top \tag{8}$$

and the quaternion product is defined as (Egeland and Gravdahl, 2002)

$$\mathbf{q}_1 \otimes \mathbf{q}_2 \triangleq \begin{bmatrix} \eta_1\eta_2 - \boldsymbol{\epsilon}_1^\top\boldsymbol{\epsilon}_2 \\ \eta_1\boldsymbol{\epsilon}_2 + \eta_2\boldsymbol{\epsilon}_1 + \mathbf{S}\left(\boldsymbol{\epsilon}_1\right)\boldsymbol{\epsilon}_2 \end{bmatrix} \tag{9}$$

2.3 *Modified Rodriguez parameters*

For control purposes we have chosen to also model the attitude using the modified Rodriguez parameters (MRP) (Shuster, 1993). This attitude representation can be defined in terms of the quaternion as

$$\boldsymbol{\sigma}_s \triangleq \frac{\boldsymbol{\epsilon}_s}{1+\eta_s}. \tag{10}$$

The MRP representation is a minimal parameter representation, and therefore contains a singularity, which can easily be identified from (10) as the point $\eta_s = -1$. The advantage when compared to other minimal representations is that the singularity is moved as far from the equilibrium as possible, that is the singularity is at $\pm 360°$. This parametrization was chosen due to the invertibility of the kinematic equation, which will be defined in the next section. A property which is crucial for our control design.

2.4 *Relative Rotational Motion*

The time derivative of a matrix $\mathbf{R}_b^a$ as in (4) can according to (Egeland and Gravdahl, 2002) be written as

$$\dot{\mathbf{R}}_b^a = \mathbf{S}\left(\boldsymbol{\omega}_{a,b}^a\right)\mathbf{R}_b^a = \mathbf{R}_b^a\mathbf{S}\left(\boldsymbol{\omega}_{a,b}^b\right) \tag{11}$$

where $\boldsymbol{\omega}_{a,b}^b$ is the angular velocity of frame b relative to frame a represented in frame b and $\mathbf{S}\left(\cdot\right)$ is the cross product operator described in (7). The kinematic differential equations for a spacecraft in its orbit frame can be found from (11) together with (5) as

$$\dot{\mathbf{q}}_s = \mathbf{T}\left(\mathbf{q}_s\right)\boldsymbol{\omega}_{s,sb}^{sb}, \mathbf{T}\left(\mathbf{q}_s\right) = \frac{1}{2}\begin{bmatrix} -\boldsymbol{\epsilon}_s^T \\ \eta_s\mathbf{I} + \mathbf{S}\left(\boldsymbol{\epsilon}_s\right) \end{bmatrix} \tag{12}$$

where $\boldsymbol{\omega}_{s,sb}^{sb}$ is the angular velocity of the spacecraft body frame relative to the orbit frame, referenced in the body frame.

In a similar manner the kinematic differential equation can be expressed in terms of the modified Rodriguez parameters as

$$\dot{\boldsymbol{\sigma}}_s = \mathbf{G}(\boldsymbol{\sigma}_s)\boldsymbol{\omega}_{s,sb}^{sb} \tag{13}$$

where

$$\mathbf{G}(\boldsymbol{\sigma}_s) \triangleq \frac{1}{4}((1-\boldsymbol{\sigma}_s^T\boldsymbol{\sigma}_s)\mathbf{I} + 2\mathbf{S}(\boldsymbol{\sigma}_s) - \boldsymbol{\sigma}_s\boldsymbol{\sigma}_s^T) \tag{14}$$

Moreover, with the assumptions of rigid body movement, the dynamical model of a spacecraft can be found from Euler's momentum equation as

$$\mathbf{J}_s\dot{\boldsymbol{\omega}}_{i,sb}^{sb} = -\mathbf{S}\left(\boldsymbol{\omega}_{i,sb}^{sb}\right)\mathbf{J}_s\boldsymbol{\omega}_{i,sb}^{sb} + \boldsymbol{\tau}_{ds}^{sb} + \boldsymbol{\tau}_{as}^{sb} \quad (15)$$

$$\boldsymbol{\omega}_{s,sb}^{sb} = \boldsymbol{\omega}_{i,sb}^{sb} + \omega_o\mathbf{c}_2 \quad (16)$$

where $\mathbf{J}_s$ is the spacecraft inertia matrix and $\boldsymbol{\omega}_{i,sb}^{sb}$ is the angular velocity of the spacecraft body frame relative to the inertial frame, expressed in the body frame. The parameter ω_o is the orbit angular velocity, $\boldsymbol{\tau}_d^{sb}$ is the disturbance torque, $\boldsymbol{\tau}_a^{sb}$ is the actuator torque, and $\mathbf{c}_2$ is the directional cosine vector from (4).

Further, by expressing the relations in (12) and (15)-(16) for both the leader and the follower spacecraft, and defining the quaternion describing the relative rotation as

$$\mathbf{q} \triangleq \bar{\mathbf{q}}_l \otimes \mathbf{q}_{l,f} \otimes \mathbf{q}_f, \quad (17)$$

where $\mathbf{q}_{l,f}$ is describes the rotation between the leader and follower body frames, the relative attitude kinematics can be expressed as (Fjellstad and Fossen, 1994)

$$\dot{\mathbf{q}} = \begin{bmatrix} \dot{\eta} \\ \dot{\boldsymbol{\epsilon}} \end{bmatrix} = \mathbf{T}(\mathbf{q})\,\boldsymbol{\omega} \quad (18)$$

where

$$\boldsymbol{\omega} = \boldsymbol{\omega}_{i,fb}^{fb} - \mathbf{R}_{lb}^{fb}\boldsymbol{\omega}_{i,lb}^{lb} \quad (19)$$

is the relative angular velocity between the leader body reference frame and the follower body reference frame. Moreover, from (19) the relative attitude dynamics can be expressed as

$$\begin{aligned}\mathbf{J}_f\dot{\boldsymbol{\omega}} &= \mathbf{J}_f\dot{\boldsymbol{\omega}}_{i,fb}^{fb} - \mathbf{J}_f\dot{\mathbf{R}}_{lb}^{fb}\boldsymbol{\omega}_{i,lb}^{lb} - \mathbf{J}_f\mathbf{R}_{lb}^{fb}\dot{\boldsymbol{\omega}}_{i,lb}^{lb} \\ &= \mathbf{J}_f\dot{\boldsymbol{\omega}}_{i,fb}^{fb} - \mathbf{J}_f\mathbf{S}\left(\boldsymbol{\omega}_{i,lb}^{fb}\right)\boldsymbol{\omega} - \mathbf{J}_f\mathbf{R}_{lb}^{fb}\dot{\boldsymbol{\omega}}_{i,lb}^{lb}\end{aligned} \quad (20)$$

where (11) and the facts that $\boldsymbol{\omega}_{lb,fb}^{fb} = \boldsymbol{\omega}$ and $\mathbf{S}(\mathbf{a})\,\mathbf{b} = -\mathbf{S}(\mathbf{b})\,\mathbf{a}, \quad \forall \mathbf{a},\mathbf{b} \in \mathcal{R}^3$ have been used. Insertion of (15), evaluated for both the leader and follower, into (20) results in (Kristiansen *et al.*, 2006)

$$\mathbf{J}_f\dot{\boldsymbol{\omega}} + \mathbf{C}_r(\boldsymbol{\omega})\,\boldsymbol{\omega} + \mathbf{n}_r(\boldsymbol{\omega}) = \boldsymbol{\Upsilon}_d + \boldsymbol{\Upsilon}_a \quad (21)$$

where

$$\begin{aligned}\mathbf{C}_r(\boldsymbol{\omega}) = &\, \mathbf{J}_f\mathbf{S}\left(\mathbf{R}_{lb}^{fb}\boldsymbol{\omega}_{i,lb}^{lb}\right) + \mathbf{S}\left(\mathbf{R}_{lb}^{fb}\boldsymbol{\omega}_{i,lb}^{lb}\right)\mathbf{J}_f \\ &- \mathbf{S}\left(\mathbf{J}_f\left(\boldsymbol{\omega} + \mathbf{R}_{lb}^{fb}\boldsymbol{\omega}_{i,lb}^{lb}\right)\right)\end{aligned} \quad (22)$$

is a skew-symmetric matrix, $\mathbf{C}_r(\boldsymbol{\omega}) \in SS(3)$,

$$\begin{aligned}\mathbf{n}_r(\boldsymbol{\omega}) = &\, \mathbf{S}\left(\mathbf{R}_{lb}^{fb}\boldsymbol{\omega}_{i,lb}^{lb}\right)\mathbf{J}_f\mathbf{R}_{lb}^{fb}\boldsymbol{\omega}_{i,lb}^{lb} \\ &- \mathbf{J}_f\mathbf{R}_{lb}^{fb}\mathbf{J}_l^{-1}\mathbf{S}\left(\boldsymbol{\omega}_{i,lb}^{lb}\right)\mathbf{J}_l\boldsymbol{\omega}_{i,lb}^{lb}\end{aligned} \quad (23)$$

is a nonlinear term, and

$$\boldsymbol{\Upsilon}_d = \boldsymbol{\tau}_{df}^{fb} - \mathbf{J}_f\mathbf{R}_{lb}^{fb}\mathbf{J}_l^{-1}\boldsymbol{\tau}_{dl}^{lb}, \quad (24)$$

$$\boldsymbol{\Upsilon}_a = \boldsymbol{\tau}_{af}^{fb} - \mathbf{J}_f\mathbf{R}_{lb}^{fb}\mathbf{J}_l^{-1}\boldsymbol{\tau}_{al}^{lb} \quad (25)$$

are the relative disturbance torques and relative actuator torques, respectively.

3. CONTROL DESIGN

In this paper we consider coordinated control of a two-satellite formation, where the control objective is to have the relative attitude track a desired time-varying smooth trajectory.

We define the error between the relative attitude and the desired relative attitude in quaternion notation as

$$\mathbf{q}_e = \mathbf{q}_d^{-1} \otimes \mathbf{q}, \quad (26)$$

which has a corresponding modified rodriguez parameter

$$\boldsymbol{\sigma}_e \triangleq \frac{\boldsymbol{\epsilon}_e}{1+\eta_e}, \quad (27)$$

with kinematic differential equation

$$\dot{\boldsymbol{\sigma}}_e = \mathbf{G}(\boldsymbol{\sigma}_e)\boldsymbol{\omega}_e, \quad (28)$$

where $\boldsymbol{\omega}_e \triangleq \boldsymbol{\omega} - \mathbf{R}(\mathbf{q}_e)\boldsymbol{\omega}_d$and $\mathbf{G}(\boldsymbol{\sigma}_e)$ is given by (14).

For controller design we use the backstepping procedure. The first step is to augment our system with a state equal to the integral of our selected error variable, to implement integral action and resistance to unknown constant perturbations. We select this state as the first backstepping variable,

$$\mathbf{z}_0 \triangleq \int_{t_0}^{t} \boldsymbol{\sigma}_e d\tau, \quad (29)$$

with the trivial dynamics

$$\dot{\mathbf{z}}_0 = \boldsymbol{\sigma}_e. \quad (30)$$

We select $\boldsymbol{\sigma}_e$ as the virtual input, defined as

$$\boldsymbol{\sigma}_e \triangleq \boldsymbol{\alpha}_0 + \mathbf{z}_1, \quad (31)$$

where $\boldsymbol{\alpha}_0$ is a stabilizing control for the $\mathbf{z}_0$-dynamics to be defined, and $\mathbf{z}_1$ is the next backstepping variable. Moreover we define the first Lyapunov function candidate

$$V_0 = \tfrac{1}{2}\mathbf{z}_0^T\mathbf{z}_0, \quad (32)$$

with derivative along the system trajectories

$$\dot{V}_0 = \mathbf{z}_0^T\dot{\mathbf{z}}_0 = \mathbf{z}_0^T(\boldsymbol{\alpha}_0 + \mathbf{z}_1). \quad (33)$$

Taking the stabilizing function as

$$\boldsymbol{\alpha}_0 = -\mathbf{K}_0\mathbf{z}_0, \quad (34)$$

where $\mathbf{K}_0 = \mathbf{K}_0^T > 0$, we obtain

$$\dot{V}_0 = -\mathbf{z}_0^T\mathbf{K}_0\mathbf{z}_0 + \mathbf{z}_1^T\mathbf{z}_0. \quad (35)$$

We proceed to define the $\mathbf{z}_1$-dynamics, using (31), as

$$\dot{\mathbf{z}}_1 = \dot{\boldsymbol{\sigma}}_e - \dot{\boldsymbol{\alpha}}_0 = \mathbf{G}\boldsymbol{\omega}_e - \dot{\boldsymbol{\alpha}}_0, \quad (36)$$

and select $\boldsymbol{\omega}_e$ as the virtual input. The virtual input is defined

$$\boldsymbol{\omega}_e = \boldsymbol{\alpha}_1 + \mathbf{z}_2. \tag{37}$$

As in the preceding step we define a Lyapunov function candidate

$$V_1 = V_0 + \frac{1}{2}\mathbf{z}_1^T\mathbf{z}_1, \tag{38}$$

with derivative along the system trajectories

$$\dot{V}_1 = -\mathbf{z}_0^T\mathbf{K}_1\mathbf{z}_0 + \mathbf{z}_1^T(\mathbf{z}_0 - \dot{\boldsymbol{\alpha}}_0 + \mathbf{G}\boldsymbol{\omega}_e). \tag{39}$$

The stabilizing function for the second backstepping subsystem is selected as

$$\boldsymbol{\alpha}_1 \triangleq \mathbf{G}^{-1}(-\mathbf{K}_1\mathbf{z}_1 + \dot{\boldsymbol{\alpha}}_0 - \mathbf{z}_0), \tag{40}$$

where $\mathbf{K}_1 = \mathbf{K}_1^T > 0$, and obtain

$$\dot{V}_1 = -\mathbf{z}_0^T\mathbf{K}_0\mathbf{z}_0 - \mathbf{z}_1\mathbf{K}_1\mathbf{z}_1 + \mathbf{z}_1^T\mathbf{G}\mathbf{z}_2 \tag{41}$$

Remark 1. In this step we take advantage of the crucial property that $\mathbf{G}^{-1}(\boldsymbol{\sigma}_e)$ is well defined for all $\boldsymbol{\sigma}_e$.

The dynamics governing the $\mathbf{z}_2$-dynamics is obtained through differentiation of (37) and insertion of (20)

$$\begin{aligned}\mathbf{J}_f\mathbf{z}_2 &= \mathbf{J}_f\dot{\boldsymbol{\omega}}_e - \mathbf{J}_f\dot{\boldsymbol{\alpha}}_1 \\ &= \mathbf{J}_f\dot{\boldsymbol{\omega}} - \mathbf{J}_f\frac{d}{dt}(\mathbf{R}(\mathbf{q}_e)\boldsymbol{\omega}_d) - \mathbf{J}_f\dot{\boldsymbol{\alpha}}_1 \\ &= -\mathbf{C}_r(\boldsymbol{\omega})\boldsymbol{\omega} - \mathbf{n}_r(\boldsymbol{\omega}) + \boldsymbol{\Upsilon}_a \\ &\quad - \mathbf{J}_f\frac{d}{dt}(\mathbf{R}(\mathbf{q}_e)\boldsymbol{\omega}_d) - \mathbf{J}_f\dot{\boldsymbol{\alpha}}_1. \end{aligned} \tag{42}$$

We continue to define a Lyapunov function candidate

$$V_2 = V_1 + \frac{1}{2}\mathbf{z}_2\mathbf{J}\mathbf{z}_2, \tag{43}$$

with derivative along the system trajectories

$$\begin{aligned}\dot{V}_2 = &-\mathbf{z}_0\mathbf{K}_0\mathbf{z}_0 - \mathbf{z}_1\mathbf{K}_1\mathbf{z}_1 + \mathbf{z}_2^T\{\mathbf{G}^T\mathbf{z}_1 \\ &- \mathbf{C}_r(\boldsymbol{\omega})\boldsymbol{\omega} - \mathbf{n}_r(\boldsymbol{\omega}) + \boldsymbol{\Upsilon}_a \\ &- \mathbf{J}_f\frac{d}{dt}(\mathbf{R}(\mathbf{q}_e)\boldsymbol{\omega}_d) - \mathbf{J}_f\dot{\boldsymbol{\alpha}}_1\}\end{aligned} \tag{44}$$

Assuming that the leader is perfectly controlled, we design the control input to the follower as

$$\begin{aligned}\boldsymbol{\tau}_f \triangleq &-\mathbf{G}^T\mathbf{z}_1 + \mathbf{C}_r(\boldsymbol{\omega})\boldsymbol{\omega} + \mathbf{n}_r(\boldsymbol{\omega}) \\ &+ \mathbf{J}_f\frac{d}{dt}(\mathbf{R}(\mathbf{q}_e)\boldsymbol{\omega}_d - \mathbf{K}_2\mathbf{z}_2\end{aligned} \tag{45}$$

which results in

$$V_2 = -\mathbf{z}_0\mathbf{K}_0\mathbf{z}_0 - \mathbf{z}_1\mathbf{K}_1\mathbf{z}_1 - \mathbf{z}_2\mathbf{K}\mathbf{z}_2. \tag{46}$$

Proposition 1. The closed-loop error dynamics

$$\dot{\mathbf{z}}_0 = -\mathbf{K}_0\mathbf{z}_0 + \mathbf{z}_1 \tag{47}$$

$$\dot{\mathbf{z}}_1 = -\mathbf{K}_1\mathbf{z}_1 - \mathbf{z}_0 + \mathbf{z}_2 \tag{48}$$

$$\dot{\mathbf{z}}_2 = -\mathbf{K}_2\mathbf{z}_2 - \mathbf{z}_1 \tag{49}$$

obtained through the backstepping procedure, is globally exponentially stable (GES), resulting in exponential convergence of the relative attitude tracking error $(\boldsymbol{\sigma}_e, \boldsymbol{\omega}_e) \to (0, 0)$.

Proof. The GES property of the closed loop dynamics (47)-(49), follows from the the final Lyapunov function candidate (43) and its derivative (46). It is clearly positive definite and decresent, and $V_2 = \mathbf{z}^T\mathbf{P}\mathbf{z}$ with $\mathbf{z} = [\mathbf{z}_0^T, \mathbf{z}_1^T, \mathbf{z}_2^T]^T$ and $\mathbf{P} = \mathrm{diag}(\mathbf{I}, \mathbf{I}, \mathbf{J}_f)$. From (46) it is clear that $\dot{V}_2$ is negative definite, and $\dot{V}_2 = -\mathbf{z}^T\mathbf{Q}\mathbf{z}$ with $\mathbf{Q} = \mathrm{diag}(\mathbf{K}_0, \mathbf{K}_1, \mathbf{K}_2)$. It is now straightforward to invoke standard Lyapunov theorems (Khalil, 2002), concluding global exponential stability of the obtained error dynamics. That is $[\mathbf{z}_0^T, \mathbf{z}_1^T, \mathbf{z}_2^T]^T$ approaches zero exponentially. Moreover we have that $\mathbf{z}_0 \equiv 0$ and $\mathbf{z}_1 \equiv 0 \Rightarrow \boldsymbol{\sigma}_e \equiv \boldsymbol{\alpha}_0 \equiv -\mathbf{K}_0\mathbf{z}_0 \equiv 0$, and $\mathbf{z}_2 \equiv 0 \Rightarrow \boldsymbol{\omega}_e \equiv \boldsymbol{\alpha}_1 \equiv 0$.

■

Remark 2. Our result is global in the sense that for any initial condition, $(\boldsymbol{\sigma}_e, \boldsymbol{\omega}_e) \to (0, 0)$ exponentially. However since we are using a minimal attitude representation, a singularity will be introduced at some level. In this case, the singularity is moved to the translation from quaternion error to modified rodriguez parameters, since the quaternion $[-1, \mathbf{0}^T]^T$ does not have a well defined MRP vector.

4. SIMULATIONS

We here present the simulation of a two-satellite formation. The leader satellite is controlled by a exponentially stable tracking controller, while the follower is controlled by the proposed controller to track a desired relative orientation.

The moment of inertia of both spacecraft are $\mathbf{J} = \mathrm{diag}(4, 3.9, 0.3)$ and the initial orientation are $\mathbf{q}_f = [0.21260.67440.6744 - 0.2126]$ for follower.

For simplicity the desired relative orientation is given as a sinusoidal signal in euler angles, given by

$$\boldsymbol{\Psi}_d = [\tfrac{25\pi}{180}\sin(\tfrac{2\pi}{500}), \tfrac{60\pi}{180}\sin(\tfrac{2\pi}{400}), \tfrac{-60\pi}{180}\sin(\tfrac{2\pi}{400})]^T. \tag{50}$$

4.1 *Results*

The simulations results for relative orientation tracking is presented in Fig. 3, with the corresponding transient error plot in Fig. 2.

As determined by the theoretical results, the relative orientation converge exponentially to the desired reference trajectory.

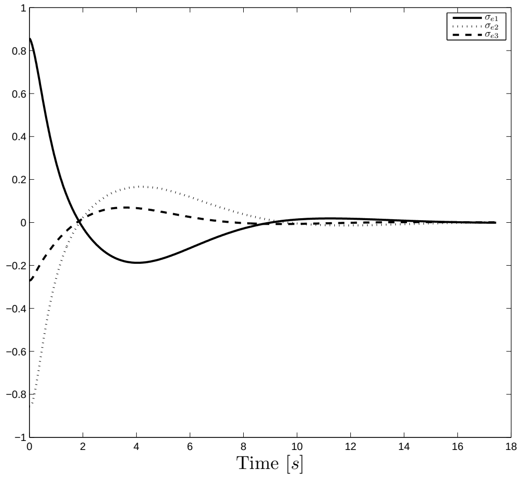

Fig. 2. Transient error expressed in modified Rodriguez parameters.

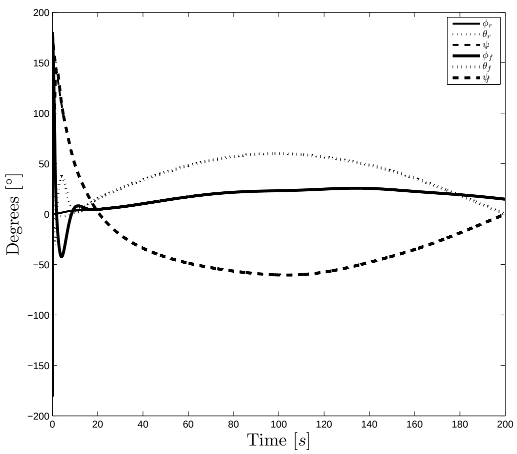

Fig. 3. Tracking of desired relative attitude, expressed in euler angles.

5. CONCLUSION

In this paper we have presented controller for the relative spacecraft attitude, including integral action to counter unmodeled constant and slowly varying disturbances. The error-dynamics has been proven to be globally exponentially stable.

6. REFERENCES

Balch, T. and R. C. Arkin (1998). Behavior-based formation control for multirobot teams. *IEEE Transactions on Robotics and Automation*.

Beard, R. W., J. R. T. Lawtond and F. Y. Hadaegh (2001). A coordination architecture for formation control. *IEEE Transactions on Control Systems Technology* **9**, 777–790.

Egeland, O. and J. T. Gravdahl (2002). *Modeling and Simulation for Automatic Control*. Marine Cybernetics. Trondheim.

Fjellstad, O.-E. and T. I. Fossen (1994). Position and attitude tracking of auv's: a quaternion feedback approach. *Oceanic Engineering, IEEE Journal of* **19**(4), 512–518.

Fossen, T.I. (2002). *Marine Control Systems: Guidance, Navigation, and Control of Ships, Rigs and Underwater Vehicles*. Marine Cybernetics.

Hughes, P. C. (1986). *Spacecraft attitude dynamics*. John Wiley & Sons. New York.

Kang, W. and H. Yeh (2002). Co-ordinated attitude control of multi-satellite systems. *International Journal of Robust and Nonlinear Control* **12**, 185–205.

Khalil, H.K. (2002). *Nonlinear Systems*. 3 ed.. Prentice Hall. Upper Saddle River, New Jersey.

Kristiansen, R., E. I. Grøtli, P. J. Nicklasson and J. T. Gravdahl (2006). A model of relative translation and rotation in leader-follower spacecraft formations. *Accepted for publication in Modeling, Identification and Control*.

Lawton, J. R. T. (2000). A Behavior-Based Approach to Multiple Spacecraft Formation Flying. PhD thesis. Bringham Young University, Dept. of El. and Comp. Engineering.

Lewis, M. A. and K. Tan (1997). High precision formation control of mobile robots using virtual structures. *Autonomous Robots* **4**, 387–403.

Mali, A. D. (2002). On the behavior-based architectures of autonomous agency. *IEEE Transactions on Systems, Man and Cybernetics, Part C: Applications and Reviews*.

Nijmeijer, H. and A. Rodriguez-Angeles (2003). *Synchronization of Mechanical Systems*. World Scientific. Singapore.

Pan, H. and V. Kapila (2001). Adaptive nonlinear control for spacecraft formation flying with coupled translational and attitude dynamics. In: *Proceedings of the 40st IEEE Conference on Decision and Control*.

Ren, W. and R. W. Beard (2004). Formation feedback control for multiple spacecraft via virtual structures. In: *2004 IEEE Proceedings of Control Theory Application*.

Schaub, H. and J. L. Junkins (2003). *Analytical Mechanics of Space Systems*. AIAA Education Series. American Institute of Aeronautics and Astronautics. Reston, VA.

Shuster, Malcolm D. (1993). A survey of attitude representations. *The Journal of the Astronautical Sciences* **41**(4), 439–517.

Sidi, M. J. (1997). *Spacecraft Dynamics & Control: A Practical Engineering Approach*. Cambridge University Press.

Tsiotras, Panagiotis (1996). Stabilization and optimality results for the attitude control problem. *Journal of Guidance, Control, and Dynamics* **19**(4), 772–779.